

Using Multilevel Circulant Matrix Approximate to Speed Up Kernel Logistic Regression

Junna Zhang, Shuisheng Zhou, Cui Fu and Zhuan Zhang,

Abstract—Kernel logistic regression (KLR) is a classical nonlinear classifier in statistical machine learning. Newton method with quadratic convergence rate can solve KLR problem more effectively than the gradient method. However, an obvious limitation of Newton method for training large-scale problems is the $O(n^3)$ time complexity and $O(n^2)$ space complexity, where n is the number of training instances. In this paper, we employ the multilevel circulant matrix (MCM) approximate kernel matrix to save in storage space and accelerate the solution of the KLR. Combined with the characteristics of MCM and our ingenious design, we propose an MCM approximate Newton iterative method. We first simplify the Newton direction according to the semi-positivity of the kernel matrix and then perform a two-step approximation of the Newton direction by using MCM. Our method reduces the time complexity of each iteration to $O(n \log n)$ by using the multidimensional fast Fourier transform (mFFT). In addition, the space complexity can be reduced to $O(n)$ due to the built-in periodicity of MCM. Experimental results on some large-scale binary and multi-classification problems show that our method makes KLR scalable for large-scale problems, with less memory consumption, and converges to test accuracy without sacrifice in a shorter time.

Index Terms—Multilevel circulant matrix, kernel logistic regression, Newton method, large-scale problem, kernel matrix approximation

I. INTRODUCTION

KERNEL logistic regression (KLR) is a log-linear model with direct probabilistic interpretation and can be naturally extended to multi-class classification problems. It is widely used in many fields, including data mining, automatic disease diagnosis, economic forecasting, etc. With the explosive growth of data scale, the space and time costs of solving KLR have become unbearable.

A number of researchers have been working to make KLR feasible for large-scale problems [1]–[3]. Existing fast solving methods mainly start from two aspects: sparsity of solutions or decomposing the original problem into subproblems. Inspired by the sparsity of support vector machine (SVM), Zhu and Hastie [1] proposed the the import vector machine (IVM) algorithm. IVM reduces the time complexity of the binary classification of KLR to $O(n^2 s^2)$, where s is the number of import points. IVM is still difficult to calculate for large-scale problems although the complexity has been reduced. Inspired by sequence minimum optimization algorithm (SMO) solving

Manuscript received XX, 2021. This work was supported by the National Natural Science Foundation of China under Grant 61772020. (Corresponding author: Shuisheng Zhou.)

J. Zhang, S. Zhou, C. Fu and Z. Zhang are with the School of Mathematics and Statistics, Xidian University, Xi'an 710071, China (e-mail: sszhou@mail.xidian.edu.cn).

SVM, Keerthi et al. [3] proposed a fast dual algorithm for solving KLR. The fast dual algorithm continuously decomposes the original problem into subproblems and only solves two variables in the subproblems. However, the introduction of kernel matrix calculation increases the time cost of the fast dual algorithm when solving the iteration update value. In short, existing methods still make it difficult to scale KLR to large-scale problems.

In this paper, we focus on kernel approximation to accelerate large-scale KLR inspired by the excellent performance of kernel approximation in learning problems [4]–[7]. A great deal of work has been done on kernel approximation. The commonly used kernel approximation methods include Nyström method [8]–[13], random feature [14]–[18], multi-level circulant matrix (MCM) [19]–[24], and so on.

Nyström method is the classical kernel matrix approximation, whose outstanding feature is the sampling of data before large-scale matrix operations. The sampling process can be done in many ways. He and Zhang [25] proposed a technique to generate sampling columns using the centroid generated by K-means clustering. Alaoui and Mahoney [10] proposed the approximate leverage score sampling, and two rounds of sampling were required for the whole set. The first round was uniform sampling to obtain the approximate leverage score, and the second round was leverage score sampling to obtain sampling columns. Although the error bounds are theoretically guaranteed, the inhomogeneity of the whole set may degrade the performance of the Nyström approximation [26].

The random feature is constructed randomly from a nonlinear mapping of the input space to the Hilbert space, that is, the direct approximation of the kernel function without calculating the elements in the kernel matrix. Rahimi and Recht [14] proposed random feature map of shifted invariant kernel functions based on Fourier transform. In order to speed up feature projection, Feng et al. [17] proposed structured random matrices, signed Circulant Random Matrix (CRM), to project input data. The feature mapping can be done in $O(nD \log d)$ time by using the fast Fourier Transform(FFT), where d and D represent the dimensions of the input data and the random feature space, respectively. Obviously, when d or D is very large, the feature mapping is prohibitive.

The idea of MCM approximates the kernel matrix was first proposed by Song and Xu [20] in 2010. Compared with the previous two methods, the MCM is a better choice. First, the inverse of a regularized kernel matrix can be calculated in $O(n \log n)$ time by using the multidimensional fast Fourier transform (mFFT). Second, only $O(n)$ is required to store MCM since we only need to store the first column. Third,

it is insensitive to the nonhomogeneity data sets since it does not require any sampling techniques. It is these advantages of MCM that have attracted the attention of researchers. With MCM approximation, Ding and Liao [23] first design an efficient LSSVM algorithm with $O(n \log n)$ time and theoretically analyze the effect of kernel matrix approximation on the decision function of LSSVM.

As the MCM approximation can effectively and succinctly reduce the complexity of time and space, by contrast, we choose the MCM approximation to speed up KLR.

Since Newton method [27] with quadratic convergence rate can solve KLR problem more effectively than gradient method, we hope to continue to use Newton method to solve KLR. The main work of Newton method is the calculation of Newton direction, and the Newton direction calculation is equivalent to solving a linear system. However, the MCM approximation cannot be directly used for acceleration because of the structure of the linear system itself. To this end, we have made a series of efforts. First, we simplify the Newton direction according to the semi-positive property of the kernel matrix. Second, we perform a two-step approximation for $K + n\lambda\Lambda^{-1}$: the first step, the MCM K_n is used to approximate the kernel matrix K ; the second step, we implement a simple heuristic modification to $n\lambda\Lambda^{-1}$, that is, the MCM τI is used to approximate $n\lambda\Lambda^{-1}$. Then, we propose an MCM approximate Newton iterative method. Our method reduces the time complexity of each iteration to $O(n \log n)$ by using the multidimensional fast Fourier transform (mFFT). In addition, the space complexity can be reduced to $O(n)$ due to the built-in periodicity of MCM.

The rest of the paper is organized as follows. In Section II, we give a brief introduction of KLR and MCM. In Section III, we present the MCM approximate Newton iterative method for solving KLR. The specific information on comparison methods is provided in Section IV. In Section V, we report experimental results. Section VI concludes this paper.

II. PRELIMINARIES

In this section, besides reviewing KLR and MCM, we introduce some interesting properties of MCM.

A. Kernel Logistic Regression

Given the training set $D = \{(\mathbf{x}_i, y_i)\}, i = 1, \dots, n$, where $\mathbf{x}_i \in \mathbb{R}^d$ is the input data and $y_i \in \{0, 1\}$ is the output targets corresponding to the input. The classical logistic regression model is described as follows:

$$\min_{\mathbf{w} \in \mathbb{R}^d} \frac{\lambda}{2} \mathbf{w}^\top \mathbf{w} - \frac{1}{n} (\mathbf{y}^\top \ln \mathbf{p} + (1 - \mathbf{y})^\top \ln(1 - \mathbf{p})), \quad (1)$$

where $\lambda > 0$ is the regularization parameter, $p_i = \frac{1}{1+e^{-\mathbf{w}^\top \mathbf{x}_i}}$ is the posterior probability estimation of $y_i = 1$.

By the representer theorem [28], the solution \mathbf{w} can be represented as

$$\mathbf{w} = \sum_{i=1}^n \alpha_i \varphi(\mathbf{x}_i), \quad (2)$$

where $\varphi(\mathbf{x}_i)$ is a map that maps the input \mathbf{x}_i into a higher or even infinite dimensional. Then plugging (2) in (1), we can get the KLR as follows:

$$\min_{\alpha \in \mathbb{R}^n} F(\alpha) := \frac{\lambda}{2} \alpha^\top K \alpha - \frac{1}{n} (\mathbf{y}^\top \ln \mathbf{p} + (1 - \mathbf{y})^\top \ln(1 - \mathbf{p})), \quad (3)$$

where K is the kernel matrix satisfying $K_{i,j} = \kappa(\mathbf{x}_i, \mathbf{x}_j) = \varphi(\mathbf{x}_i) \cdot \varphi(\mathbf{x}_j)$ and $\mathbf{p}_i = \frac{1}{1+e^{-\kappa(\mathbf{x}_i, \cdot)\alpha}}$, $\kappa(\mathbf{x}_i, \cdot)$ is the i -th row of the kernel matrix.

KLR is a convex optimization problem, which can be solved by Newton method [27] with quadratic convergence rate. However, Newton method requires $O(n^3)$ time complexity and $O(n^2)$ space complexity for each iteration, which is not feasible for large-scale data sets. Therefore, we need a more effective method to solve KLR.

B. Multilevel Circulant Matrix Approximation

To better understand the MCM approximation, we need to introduce the concept of MCM and some of its interesting properties, and analyze its computational advantages.

To facilitate representation, we introduce the notion of multilevel indexing. Let \mathbb{N} be a set of positive integers. For $n \in \mathbb{N}$, let $[n] := \{0, 1, \dots, n-1\}$. For a positive integer p and $\mathbf{n} := [n_0, n_1, \dots, n_{q-1}] \in \mathbb{N}^q$. We denote

$$n = n_0 n_1 \cdots n_{q-1}, \quad (\text{continued product})$$

$$[\mathbf{n}] := [n_0] \times [n_1] \times \cdots \times [n_{q-1}] \in \mathbb{R}^{n \times q}, \quad (\text{Cartesian product})$$

where $[\mathbf{n}]$ represents a set of multilevel indexing.

An MCM is a matrix that can be partitioned into blocks which are further partitioned into smaller blocks, and possibly so on. According to [29], a matrix K_n is called a q -level circulant matrix of level order \mathbf{n} if it consists of $n_0 \times n_0$ blocks and each block is a $(q-1)$ -level circulant matrix of level order $[n_0, n_1, \dots, n_{q-1}]$. Specifically, $K_n = [K_{i,j} : i, j \in [\mathbf{n}]]$ is called a q -level circulant matrix if for any $i \in [\mathbf{n}], j \in [\mathbf{n}]$,

$$K_{i,j} = \mathbf{k}_i - \text{mod}(j_0, n_0), \dots, i_{q-1} - \text{mod}(j_{q-1}, n_{q-1}),$$

where \mathbf{k}_i is the first column of K_n . Then a q -level circulant matrix K_n is fully determined by its first column. So we write $K_n = \text{circ}_{\mathbf{n}}[\mathbf{k}_i : i \in [\mathbf{n}]]$, where $\mathbf{k}_i = \mathbf{k}_{i,0}$ for $i \in [\mathbf{n}]$.

We further introduce the properties of MCM [30], which help us to explore the computational advantages of MCM.

Lemma 1. Suppose that K_n is an MCM of level order \mathbf{n} and \mathbf{k} is the first column of K_n . Then K_n is a q -level circulant matrix of level order \mathbf{n} if and only if

$$K_n = \frac{1}{n} \phi^* \text{diag}(\phi \mathbf{k}) \phi, \quad (4)$$

where $\phi = F_{n_0} \otimes F_{n_1} \otimes \cdots \otimes F_{n_{q-1}}$, \otimes denotes the Kronecker product of matrices and $F_n = [e^{(2\pi i/n_{q-j})st} : s, t \in [n_{q-j}]]$, $j = 1, 2, \dots, q$ with i being the imaginary unit.

Theorem 1. Assume that A_n and B_n are both MCM of level order \mathbf{n} , \mathbf{a} and \mathbf{b} are the first columns of A_n and B_n respectively, then $C_n = A_n + B_n$ is an MCM of level order \mathbf{n} , and $\mathbf{a} + \mathbf{b}$ is the first column of C_n .

Proof. From Lemma 1, A_n and B_n can be represented as

$$A_n = \frac{1}{n} \phi^* \text{diag}(\phi \mathbf{a}) \phi, B_n = \frac{1}{n} \phi^* \text{diag}(\phi \mathbf{b}) \phi.$$

It follows that:

$$C_n = A_n + B_n = \frac{1}{n} \phi^* \text{diag}(\phi(\mathbf{a} + \mathbf{b})) \phi.$$

According to Lemma 1, C_n is an MCM of level order \mathbf{n} , and $\mathbf{a} + \mathbf{b}$ is the first column of C_n . \square

Theorem 2. Assume that A_n is an invertible MCM of level order \mathbf{n} and \mathbf{a} is the first column of A_n , then A_n^{-1} is also an MCM, and $A_n^{-1} = \frac{1}{n} \phi^* \text{diag}(\frac{1}{\phi \mathbf{a}}) \phi$.

Now we introduce Algorithm 1 to construct an MCM from a kernel function. From [22], we can generate an MCM K_n as the approximation of kernel matrix K .

Algorithm 1 Construction of an MCM

Input: a kernel function κ , a sequence of positive numbers $\mathbf{h} = (h_0, h_1, \dots, h_{q-1}) \in \mathbb{R}^q$, level order $\mathbf{n} \in \mathbb{N}^q$.

Output: K_n .

- 1: Calculate $\mathbf{t}_i = \kappa(|\mathbf{i}_s \mathbf{h}_s : s \in [q]|_2)$, $\forall \mathbf{i} \in [\mathbf{n}]$.
- 2: Let $D_{i,s} = \begin{cases} \{0\}, & \mathbf{i}_s = 0, \\ \{\mathbf{i}_s, \mathbf{n}_s - \mathbf{i}_s\}, & 1 \leq \mathbf{i}_s \leq \mathbf{n}_s - 1, \end{cases}$ and $D_i = D_{i,0} \times D_{i,1} \times \dots \times D_{i,q-1}$, $\forall \mathbf{i} \in [\mathbf{n}]$ and $\forall s \in [q]$.
- 3: Calculate $\mathbf{k}_i = \sum_{j \in D_i} \mathbf{t}_j$.
- 4: **return** $K_n = \text{circ}_n[\mathbf{k}_i : i \in [\mathbf{n}]]$.

For K_n generated by Algorithm 1, only $O(n)$ is required to store it since we only need to store the first column. By Lemma 1, $K_n \mathbf{x}$ is equivalent to implementing $\frac{1}{n} \phi^* \text{diag}(\phi \mathbf{k}) \phi \mathbf{x}$, which can be realized efficiently in $O(n \log n)$ time complexity using the mFFT. According to Theorem 2, $K_n^{-1} \mathbf{x}$ is equivalent to implementing $\frac{1}{n} \phi^* \text{diag}(\frac{1}{\phi \mathbf{k}}) \phi \mathbf{x}$, which also can be realized efficiently in $O(n \log n)$ time complexity. In addition to its advantages in computation and space storage, MCM approximation also does not require any sampling techniques. Next, we will design a faster and more effective method to solve KLR based on MCM.

III. MCM APPROXIMATE NEWTON ITERATIVE METHOD

In this section, we first simplify the Newton direction based on the positive semidefiniteness of K , and then use MCM to approximate the simplified Newton direction. Finally, we propose the MCM approximation of Newton method.

A. Simplified Newton Direction

KLR is a convex optimization problem [31], and the local optimal solution must be the global optimal solution. For convex optimization problems, Newton method with at least quadratic convergence can be used to solve them. The gradient and Hessian are obtained by differentiating (3) with respect to α . The gradient is

$$\nabla F(\alpha) = -\frac{1}{n} K^\top (\mathbf{y} - \mathbf{p}) + \lambda K \alpha, \quad (5)$$

the Hessian of (3) is as follows:

$$\nabla^2 F(\alpha) = \frac{1}{n} K^\top \Lambda K + \lambda K, \quad (6)$$

where Λ is a diagonal matrix whose elements are $\mathbf{p}_i(1 - \mathbf{p}_i)$, $i = 1, \dots, n$. Based on the (5) and (6), we obtain the corresponding Newton direction as follows:

$$\mathbf{d} = (K^\top \Lambda K + n\lambda K)^{-1} (K^\top (\mathbf{y} - \mathbf{p}) - n\lambda K \alpha) \quad (7)$$

Obviously, in order to compute the Newton direction, we need to perform an inverse on an $n \times n$ matrix in each iteration and the time complexity is $O(n^3)$. This kind of scalability is prohibitive for large-scale problems. In order to make it feasible, we propose the simplified Newton direction and prepare for the subsequent MCM matrix approximation.

We rewrite (7) as follows:

$$(K^\top \Lambda K + n\lambda K) \mathbf{d} = K^\top (\mathbf{y} - \mathbf{p}) - n\lambda K \alpha. \quad (8)$$

Since the kernel matrix is symmetric, we have

$$K(\Lambda K + n\lambda I) \mathbf{d} = K(\mathbf{y} - \mathbf{p} - n\lambda \alpha). \quad (9)$$

If the kernel matrix K is positive definite, we have

$$(\Lambda K + n\lambda I) \mathbf{d} = \mathbf{y} - \mathbf{p} - n\lambda \alpha. \quad (10)$$

If the kernel matrix K is positive semidefinite, then the solution to (9) is not necessarily unique, but the unique solution of (10) is the solution of (9). Therefore, we can use the solution of (10) as the Newton direction.

Due to the positive definiteness of Λ and the positive semidefiniteness of K , the invertibility of $\Lambda K + n\lambda I$ can be guaranteed by setting $\lambda > 0$. So, we can get the simplified Newton direction as follows:

$$\begin{aligned} \mathbf{d} &= (\Lambda K + n\lambda I)^{-1} (\mathbf{y} - \mathbf{p} - n\lambda \alpha) \\ &= (K + n\lambda \Lambda^{-1})^{-1} \Lambda^{-1} (\mathbf{y} - \mathbf{p} - n\lambda \alpha). \end{aligned} \quad (11)$$

B. Approximate Newton Direction using MCM

Here, based on the nice properties of MCM, we propose the idea of approximating Newton direction by MCM.

Replacing K with K_n generated by Algorithm 1 in (11), we can obtain the approximate Newton direction as follows:

$$\bar{\mathbf{d}} = (K_n + n\lambda \Lambda^{-1})^{-1} \Lambda^{-1} (\mathbf{y} - \tilde{\mathbf{p}} - n\lambda \alpha), \quad (12)$$

where $\tilde{\mathbf{p}} = \frac{1}{1+e^{-K_n \alpha}}$.

Naturally, we can consider (12) as a large-scale linear system, and then obtain an approximate solution of Newton direction by the conjugate gradient method [32]. The conjugate gradient method converges after n iterations at most, and because of the use of mFFT during the iterations, it allows us to obtain the approximate solution of (12) in $O(n^2 \log n)$ time much less than $O(n^3)$. However, the time complexity can be further reduced to $O(n \log n)$ by using appropriate approximation below.

Fortunately, we can use the nice properties of MCM to speed up the calculation of (12) if we can approximate $n\lambda \Lambda^{-1}$ with an MCM. Such consideration drives us to find an MCM A_n to

approximate $n\lambda\Lambda^{-1}$, which is to solve the following problem:

$$\min_{A_n \in \mathbb{A}_n} \|A_n - n\lambda\Lambda^{-1}\|_F^2, \quad (13)$$

where \mathbb{A}_n is the set of MCMs of level order n .

By working out the optimality condition of the problem (13), we obtain the following proposition.

Proposition 1. *The optimal solution of the problem (13) is*

$$A_n = \tilde{\tau}I, \quad (14)$$

where $\tilde{\tau} = \lambda \sum_{i=1}^n \frac{1}{\Lambda_{ii}}$.

Proof. The first-order optimality conditions of (13) are:

$$2(A_n - n\lambda\Lambda^{-1}) = 0.$$

Taking into account the built-in periodicity of A_n , we get the optimal solution of the problem (13) is $A_n = \tilde{\tau}I$, where $\tilde{\tau} = \lambda \sum_{i=1}^n \frac{1}{\Lambda_{ii}}$. \square

Then, we further obtain the following approximate Newton direction with MCM:

$$\tilde{d} = (K_n + \tilde{\tau}I)^{-1}\Lambda^{-1}(y - \tilde{p} - n\lambda\alpha), \quad (15)$$

According to the nice properties of MCM, the time complexity of the approximate Newton direction (15) is $O(n \log n)$, which is much less than $O(n^2 \log n)$.

To illustrate the effectiveness of using $\tilde{\tau}I$ to approximate $n\lambda\Lambda^{-1}$, we have experimentally compared the two cases on six small-scale benchmark classification data sets. The detailed information of several small-scale datasets are listed in Table IV. The variation of the two-norm of the gradient are plotted in Fig. 1. In addition, Table I lists the differences in the optimal solution α obtained in these two cases.

Fig. 1 shows that the variation trend of the two-norm of the gradient obtained in the two cases of $\tilde{\tau}I$ and $n\lambda\Lambda^{-1}$ is basically the same, although on the Australian and the USPS, the number of iterations when convergence is achieved increases somewhat. Table I makes it even more clear that the optimal solutions obtained in both cases are nearly the same. Therefore, we can use $\tilde{\tau}I$ to approximate $n\lambda\Lambda^{-1}$, and then we can use mFFT to accelerate learning.

TABLE I: The difference between the optimal solution for $\tilde{\tau}I$ and $n\lambda\Lambda^{-1}$. α represents the optimal solution obtained by the former, and $\tilde{\alpha}$ represents the optimal solution obtained by the latter.

Data Sets	Ionosphere	Australian	Banknote	Titanic	Banana	USPS
$\ \alpha - \tilde{\alpha}\ _2$	2.51e-12	4.27e-09	4.00e-10	5.85e-10	1.64e-08	3.33e-05
$\ \alpha - \tilde{\alpha}\ _\infty$	4.05e-13	3.10e-09	4.09e-11	1.20e-10	7.74e-10	8.09e-05

C. MCM Approximate Newton Iterative Method

We are now ready to design MCM approximate Newton iterative method, which can reduce the time and space complexity more succinctly and effectively.

The main work of Newton method is the calculation of Newton direction. According to Theorem 1, $K_n + \tilde{\tau}I$ is an MCM. By Theorem 2, we have

$$(K_n + \tilde{\tau}I)^{-1} = \frac{1}{n} \phi^* \text{diag}\left(\frac{1}{\phi k + \tilde{\tau}}\right) \phi.$$

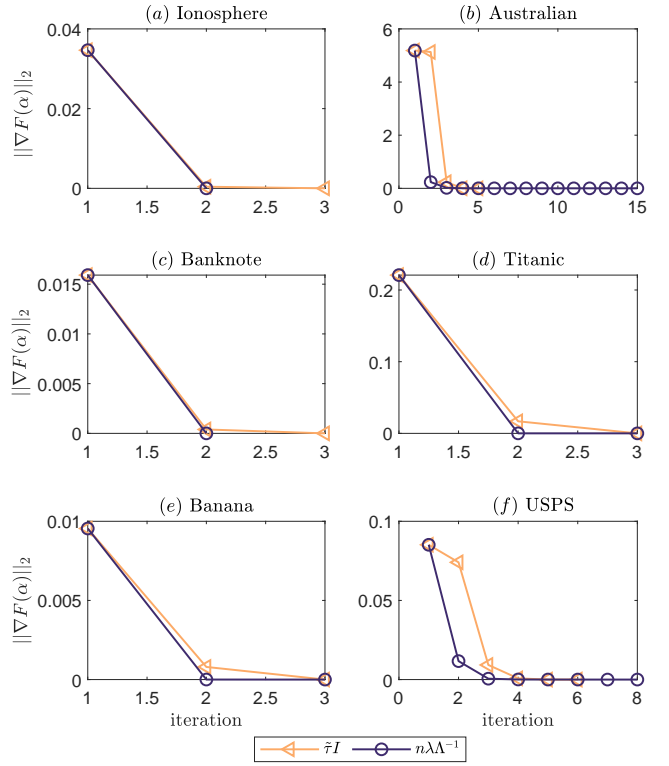


Fig. 1: Plots for the variation trend of the two-norm of the gradient with the number of iterations on six small-scale benchmark datasets.

Then we rewrite (15) as follows:

$$\tilde{d} = \frac{1}{n} \phi^* \text{diag}\left(\frac{1}{\phi k + \tilde{\tau}}\right) \phi \Lambda^{-1} (y - \tilde{p} - n\lambda\alpha). \quad (16)$$

where $\tilde{p} = \frac{1}{1+e^{-K_n\alpha}}$. In addition, replacing K with K_n generated by Algorithm 1, we can obtain the approximate values of the objective function (3) and the gradient (5) are obtained as follows:

$$\tilde{F}(\alpha) = \frac{\lambda}{2} \alpha^\top K_n \alpha - \frac{1}{n} (y^\top \ln \tilde{p} + (1-y)^\top \ln(1-\tilde{p})), \quad (17)$$

$$\nabla \tilde{F}(\alpha) = K_n (\lambda \alpha - \frac{1}{n} (y - \tilde{p})). \quad (18)$$

Now we present the detailed flow of the MCM approximate Newton iterative method in Algorithm 2.

D. Complexity Analysis

Due to the nice properties of MCM, our algorithm can reduce the time and space complexity in solving KLR more succinctly. In the following, we will study the time and space complexity of the Algorithm 2 in more detail.

1) **Space Complexity:** Because of the built-in periodicity of MCM, only $O(n)$ space storage is required. This plays an important role in the consumption of memory. Considering the fragmentation memory footprint of the other parameters, we can eventually abbreviate the space complexity of the Algorithm 2 to $O(n)$.

2) **Time Complexity:** From [19], the complexity of the step 2 is $O(n)$. We know the time complexity of steps 3,

Algorithm 2 MCM approximate Newton iterative method

Input: Data set D , parameters σ, β, R, T and ε .
Output: α .

- 1: **Initialize:** $\alpha_0 = 0, R = 10, T = 30, r = 1, t = 0, \varepsilon = 10^{-6}$.
- 2: Calculate $[k_i : i \in [n]]$ according to Algorithm 1.
- 3: Calculate $v = \phi[k_i : i \in [n]]$ by mFFT.
- 4: Calculate $\tilde{p}, \nabla \tilde{F}(\alpha_0)$ and $F(\alpha_0)$.
- 5: **while** $t \leq T$ and $\|\nabla \tilde{F}(\alpha_t)\| > \varepsilon$ **do**
- 6: Calculate $\eta = \Lambda^{-1}(y - \tilde{p} - n\lambda\alpha_t)$.
- 7: Calculate $\delta = \phi\eta$ by mFFT.
- 8: Calculate $\zeta = \text{diag}(\frac{1}{v_i + \tau}, i = 1, 2, \dots, n)\delta$.
- 9: Calculate $\tilde{d} = \frac{1}{n}\phi^*\zeta$ using inverse mFFT.
- 10: Update $\tilde{\alpha} = \alpha_t + \tilde{d}$ and calculate $\tilde{F}(\tilde{\alpha})$.
- 11: **while** $r \leq R$ and $\tilde{F}(\tilde{\alpha}) \geq \tilde{F}(\alpha_t)$ **do**
- 12: Update $\tilde{\alpha} = \alpha_t + 0.5^r \tilde{d}$ and calculate $\tilde{F}(\tilde{\alpha})$.
- 13: $r := r + 1$.
- 14: **end while**
- 15: $r = 1$.
- 16: Update $\alpha_{t+1} = \tilde{\alpha}$, calculate \tilde{p} and $\nabla \tilde{F}(\alpha_{t+1})$.
- 17: $t := t + 1$.
- 18: **end while**
- 19: **return** $\alpha \leftarrow \alpha_t$.

7 and 9 is $O(n \log n)$, since mFFT can be applied with the $O(n \log n)$ complexity. The main work of the steps 4, 10 and 16 is to calculate the form $K_n x$. According to II-B, the time complexity of the steps 4, 10 and 16 is $O(n \log n)$. The time complexity of steps 6 and 8 is $O(n)$. In the process of calculating $\tilde{F}(\tilde{\alpha})$ in the step 10, we can store $K_n \alpha_t$ and $K_n \tilde{d}$ to facilitate the calculation of $\tilde{F}(\tilde{\alpha})$ in the step 12. Then only $O(n)$ times multiplications are needed to calculate $\tilde{F}(\tilde{\alpha})$ in the step 12. Because the maximum number of iterations for outer and inner loops is T and R , respectively, the total maximum time complexity of Algorithm 2 is $O(nq + Tn \log n + TRn)$. At the same time, [19] showed that a small q (e.g., 3) is sufficient for a sufficient approximation of the classification problem. This means that we can abbreviate the time complexity of the Algorithm 2 to $O(Tn \log n)$.

IV. COMPARED METHODS

In this section, we briefly introduce several kernel approximation methods, and apply them to Newton method to solve KLR problem respectively. Finally, we analyze their time and space complexity in solving KLR.

A. Standard Nyström Method

Here, we briefly review the standard Nyström Approximation (Nys) [4]. For the kernel matrix K , we first randomly select its c columns uniformly without replacement and denote the matrix consisting of the selected columns as C . Then we use W to denote the intersection of the selected rows and columns of K . We can get the standard Nyström approximation matrix is $\tilde{K} = CW^{-1}C^\top$. Note that W may be non-positive definite, in which case the positive definiteness of W can be guaranteed by slight regularization.

The eigenvalue decomposition of W is $W = U\Sigma U^\top$, where U is a matrix composed of eigenvectors of W , Σ is a diagonal matrix, and each diagonal element is an eigenvalue of W . Now we can write the approximate matrix as follows:

$$\tilde{K} = CU\Sigma^{-1}U^\top C^\top = VV^\top, \quad (19)$$

where $V = CU\sqrt{\Sigma^{-1}}$. It can be seen from the above process that generating V requires $O(ndc + c^3)$ time.

Now we use $\tilde{K} = VV^\top$ as an approximation of K . Due to the positive definiteness of Λ and the positive semi-definiteness of \tilde{K} , we can ensure the invertibility of $\tilde{K} + n\lambda\Lambda^{-1}$. Using the Woodbury formula [33], we can obtain the approximate Newton direction as follows:

$$\begin{aligned} \tilde{d} &= (VV^\top + n\lambda\Lambda^{-1})^{-1}\Lambda^{-1}(y - \tilde{p} - n\lambda\alpha) \\ &= \frac{1}{n\lambda}\Lambda(I - \frac{1}{n\lambda}V(I_c + \frac{1}{n\lambda}V^\top\Lambda V)^{-1}V^\top\Lambda)\Lambda^{-1}(y - \tilde{p} - n\lambda\alpha), \end{aligned} \quad (20)$$

where $\tilde{p} = \frac{1}{1+e^{-VV^\top\alpha}}$, I_c is a $c \times c$ identity matrix. Similarly, the approximate values of the objective function (3) and gradient (5) are obtained as follows:

$$\tilde{F}(\alpha) = -\frac{1}{n}(y^\top \ln \tilde{p} + (1 - y)^\top \ln(1 - \tilde{p})) + \frac{\lambda}{2}\alpha^\top VV^\top\alpha, \quad (21)$$

$$\nabla \tilde{F}(\alpha) = VV^\top(\lambda\alpha - \frac{1}{n}(y - \tilde{p})). \quad (22)$$

The time complexity of calculating (20) is $O(nc^2 + c^3)$, and the time complexity of calculating (21) and (22) is $O(nc)$.

B. Recursive RLS-Nyström Method

Recursive RLS-Nyström method (RRLS-Nys) [11]¹ is sampled according to the approximate ridge leverage scores of the kernel matrix, and obtains landmark points with higher quality. Ridge leverage scores sampling not only provides a strong theoretical guarantee for Nys, but also a fast recursive sampling scheme may enable RRLS-NYS to achieve low-rank kernel approximation in a shorter time. After obtaining c sample points, the rest of the operation is the same as Nys.

C. Signed Circulant Random Feature Mapping

Signed Circulant Random Feature mapping (SCRF) [17] first uses the structured random matrix $\Pi \in \mathbb{R}^{D \times d}$, a stacking of D/d signed circulant Gaussian matrices, to project input data, and then performs a non-linear transform

$$\Phi : x \mapsto \sqrt{\frac{2}{D}} \cos(\Pi x + b),$$

where D represents the dimensionality of the random feature space, $b \in \mathbb{R}^D$ is a random vector drawn i.i.d. from $[-\pi, \pi]$ uniformly. Now we can write the approximate matrix as $\tilde{K} = \Phi\Phi^\top$. Replacing V with Φ in (20), (21) and (22), we obtain the following results:

$$\tilde{d} = \frac{1}{n\lambda}\Lambda(I - \frac{1}{n\lambda}\Phi(I_D + \frac{1}{n\lambda}\Phi^\top\Lambda\Phi)^{-1}\Phi^\top\Lambda)\Lambda^{-1}(y - \tilde{p} - n\lambda\alpha), \quad (23)$$

$$\tilde{F}(\alpha) = \frac{\lambda}{2}\alpha^\top\Phi\Phi^\top\alpha - \frac{1}{n}(y^\top \ln \tilde{p} + (1 - y)^\top \ln(1 - \tilde{p})), \quad (24)$$

¹Codes are available in <https://github.com/cnmusco/recursive-nystrom>

$$\nabla \tilde{F}(\alpha) = \Phi \Phi^\top (\lambda \alpha - \frac{1}{n} (\mathbf{y} - \tilde{\mathbf{p}})), \quad (25)$$

where $\tilde{\mathbf{p}} = \frac{1}{1+e^{-\Phi \Phi^\top \alpha}} \mathbf{1}$, I_D is a $D \times D$ identity matrix.

For the structured random matrix projection, we can compute the feature mapping in $O(D \log d)$ time by using the fast Fourier transform (FFT). Then generating Φ requires $O(nD \log d)$ time. The time complexity of calculating (23) is $O(nD^2 + D^3)$, and the time complexity of calculating (24) and (25) is $O(nD)$.

Table II shows the time and space complexity of the typical approximation method using Newton method to solve KLR.

TABLE II: Compare the typical approximate methods of solving KLR by Newton method. The space complexity of every method is in the second column. The time complexity of every method is in the third column. n denotes the number of training data, d denotes the data dimension, c denotes the number of samples, D denotes the dimensionality of the random feature space, T denotes the number of outer loop iterations, R denotes the number of inner loop iterations

Method	Space complexity	Time complexity
Original	$O(n^2)$	$O(Tn^3 + TRn^2)$
Nys	$O(nc)$	$O(T(nc^2 + c^3) + TRnc)$
RRLS-Nys	$O(nc)$	$O(T(nc^2 + c^3) + TRnc)$
SCRF	$O(nD)$	$O(T(nD^2 + D^3) + TRnD)$
This paper	$O(n)$	$O(Tn \log n)$

V. EXPERIMENT RESULTS

In this section, we conduct experiments on some binary and multi-classification datasets to evaluate the effectiveness of our algorithm. All the experiments were in MATLAB and run on a 3.6 GHz Intel Core i7 with 16GB of memory.

We compare four kernel matrix approximation methods, including the Nyström approximation, recursive RLS-Nyström approximation, signed circulant matrix projection and MCM approximation. We fixed $T = 30$, $R = 10$ and the stop criterion $\varepsilon = 10^{-6}$. Gaussian kernel function $\kappa(\mathbf{x}_i, \mathbf{x}_j) = \exp(-\sigma \|\mathbf{x}_i - \mathbf{x}_j\|^2)$, where $\sigma > 0$ is the kernel parameter. For all the experiments, there are two parameters need to be determined in advance, i.e., σ and λ . The regularization parameter λ and the kernel parameter σ listed in Table III were chosen by a cross-validation procedure and grid search with $\sigma \in \{2^{-9}, \dots, 2^{16}\}$ and $\lambda \in \{10^{-6}, \dots, 10^0\}$.

TABLE III: Parameter settings of algorithms.

Data Sets	Binary classification			Multi-class classification				
	σ	λ	Data Sets	σ	λ	Data Sets		
Ionosphere	2^2	10^{-3}	Adult	2^{-7}	10^{-3}	Shuttle	2^{15}	10^{-3}
Australian	2^{-7}	10^{-2}	Shuttle	2^{15}	10^{-3}	Sensorless	2^9	10^{-4}
Banknote	2^2	10^{-2}	Mnist	2^{-1}	10^{-5}	Connect-4	2^2	10^{-4}
Titanic	2^{-2}	10^{-1}	Vehicle	2^{-4}	10^{-1}	Mnist	2^{-1}	10^{-6}
Banana	2^3	10^{-3}	Skin	2^{11}	10^{-3}	Vehicle	2^5	10^{-3}
USPS	2^{-1}	10^{-4}	Covtype	2^9	10^{-4}	CovtypeM	2^9	10^{-4}

When setting the sample size, there is a tradeoff between time and precision. The sampling size c of the Nyström method and the recursive RLS-Nyström was set to $c = \sqrt{n}$. The dimensionality D of SCRF was set to $D = O(d)$. For MCM approximation, a 3-level circulant matrix was adopted. For simplicity, the same value for each dimension of the

parameter vector \mathbf{h} was taken; that is $\mathbf{h} = h \cdot \mathbf{1} \in \mathbb{N}^q$. According to [19], we could tune h to minimize $\|X_n - H_n\|_F$, where $X_n = [\|\mathbf{x}_i - \mathbf{x}_j\| : i, j \in [n]]$, $H_n = [h\|\mathbf{i} - \mathbf{j}\| : i, j \in [n]]$. In the experiments, we fix $h = 1$, since it is sufficient to demonstrate the validity of the Algorithm 2. To avoid randomness, all experiments are operated 10 times independently, and the mean value is set as the final result.

The first set of experiments in Section V-A, performed on some small-scale benchmark datasets. Compared with the original algorithm, our algorithm and several other approximate algorithms can obtain similar classification performance.

The second set of experiments in Section V-B was carried out on some large-scale benchmark classification datasets. Compared with other approximate algorithms, our algorithm can achieve similar or even better classification performance while spending less time.

In order to further illustrate the superiority of our algorithm, Section V-C specifically analyzes the influence of Nys and RRLS-Nys sampling column number on the classification performance of checkerboard dataset.

KLR can be naturally extended to multi-classification problems. In Section V-D, we perform multi-classification experiments on six multi-classification datasets, which shows that our algorithm has the same superiority in this case.

A. Small-scale Benchmark Datasets Experiments

In this section, we test six small-scale benchmark classification datasets to illustrate that the classification performance of the approximate algorithm is comparable to the original algorithm. For USPS, the task of classifying the digit 8 versus the rest classes was trained. The Australian and USPS datasets were downloaded from the LIBSVM [34], and the Ionosphere, Banknote, Titanic and Banana datasets were downloaded from the UCI database [35]. These datasets are detailed in Table IV.

The variation of the two-norm of the gradient are plotted in Fig. 2. Table IV reports the experimental results for the six small-scale datasets.

It can be seen from Fig. 2 that, compared with the original algorithm, several approximation methods can converge, and at the same time, the number of iterations when convergence is achieved will be reduced, except for Australian and USPS.

From Table IV, it is clear that the classification performance of the four approximation algorithms is comparable to that of the original algorithm.

B. Large-scale Benchmark Datasets Experiments

In this section, we test six large datasets of benchmark classification to further demonstrate the superiority of our algorithm. For Mnist, the task of classifying the digit 8 versus the rest classes was trained. For Vehicle, the task of classifying class 3 from the rest was trained. These datasets were downloaded from the LIBSVM [34].

The variation of the two-norm of the gradient are plotted in Fig. 3. Table V reports the experimental results for the six large-scale datasets.

From Fig. 3, the four approximate methods can reach convergence in six large-scale data sets. The convergence

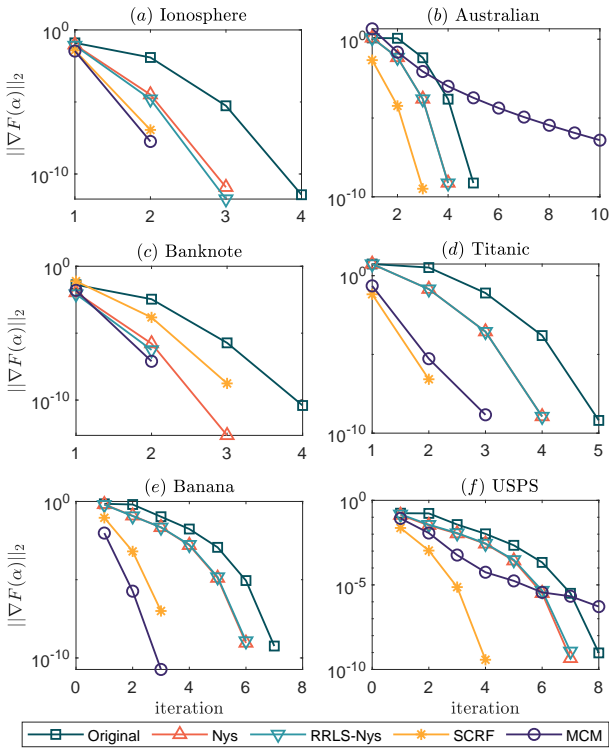


Fig. 2: Plots for the variation trend of the two-norm of the gradient with the number of iterations on the six small-scale benchmark classification datasets.

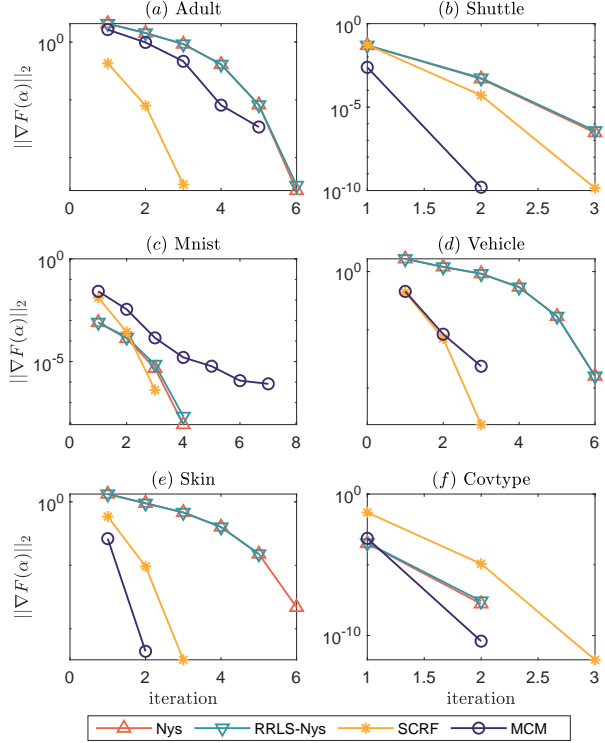


Fig. 3: Plots for the variation trend of the two-norm of the gradient with the number of iterations on the six large-scale benchmark classification datasets.

process of NYS and RRLS-NYS is basically the same. SCRF has the least number of iterations in the case of convergence, followed by MCM.

TABLE IV: Comparison of different algorithms on the six small-scale benchmark classification datasets. The standard deviations are given in brackets. 'AUC' stands for "Area under the ROC Curve". m and n are the numbers of training and testing samples respectively. d is the dimension of data.

Data Sets	Algorithms	Accuracy(%)	AUC(%)
Ionosphere $m=216$ $n=135$ $d=34$	Original	92.30	97.53(1.06)
	Nys	91.41	96.76(1.39)
	RRLS-Nys	91.41	97.71(1.13)
	SCRF	91.70	96.99(1.19)
	MCM	92.22	97.81(1.00)
Australian $m=512$ $n=178$ $d=14$	Original	85.11	92.74(2.16)
	Nys	84.89	91.89(1.80)
	RRLS-Nys	84.38	92.38(1.69)
	SCRF	56.18	92.42(2.42)
	MCM	87.64	92.54(2.19)
Banknote $m=1000$ $n=372$ $d=4$	Original	1.00	1.00(0.00)
	Nys	99.95	1.00(0.00)
	RRLS-Nys	99.95	1.00(0.00)
	SCRF	99.97	1.00(0.00)
	MCM	99.97	1.00(0.00)
Titanic $m=1331$ $n=870$ $d=3$	Original	77.41	74.75(1.00)
	Nys	77.48	74.06(1.47)
	RRLS-Nys	77.51	74.50(1.65)
	SCRF	77.87	74.67(2.30)
	MCM	77.31	73.58(1.05)
Banana $m=3430$ $n=1870$ $d=2$	Original	90.54	96.82(0.18)
	Nys	89.86	95.67(0.86)
	RRLS-Nys	89.78	95.98(0.35)
	SCRF	90.11	95.95(0.17)
	MCM	90.43	96.06(0.30)
USPS $m=7291$ $n=2007$ $d=256$	Original	99.26	98.95(0.14)
	Nys	99.25	98.83(0.24)
	RRLS-Nys	99.26	98.90(0.18)
	SCRF	99.24	98.80(0.23)
	MCM	99.13	99.33(0.14)

From Table V, we have four observations. Firstly, our algorithm's classification performance is comparable to the other three algorithms on all datasets except Adult and Vehicle. For the Adult and Vehicle, the AUC of our algorithm is slightly lower than that of the Nys and RRLS-Nys, but the training time of the Nys and RRLS-Nys is longer than our algorithm. Secondly, the performance of SCRF is slightly worse than that of Nys and RRLS-Nys, and the performance of Nys and RRLS-Nys is similar, which is consistent with the conclusions of [11]. Thirdly, the larger the dimension of training set is, the time cost of SCRF increases obviously, which is consistent with the complexity analysis. Fourthly, it can be clearly seen that the larger the training set is, the more obvious the efficiency gain of our algorithm is, which is consistent with the results of complexity analysis.

C. Checkerboard Dataset Experiments

In order to further illustrate the superiority of our algorithm, the influence of sampling column number of the Nys and RRLS-Nys on the classification performance of Checkerboard dataset is specifically analyzed in this section.

Checkerboard dataset was first proposed in [36] and later widely used to illustrate the effectiveness of nonlinear kernel method [37]–[39]. Checkerboard dataset was generated by the following method: randomly sampled 1600000 points from the regions $[0, 1] \times [0, 1]$ and labeled two classes by 4×4 XOR

TABLE V: Comparison of different algorithms on the six large-scale benchmark classification datasets. 'AUC' stands for "Area under the ROC Curve". m and n are the numbers of training and testing samples respectively. d is the dimension of data. The standard deviations are given in brackets.

Data Sets	Algorithms	Training time(s)	Accuracy (%)	AUC (%)
Adult m=32561 n=16281 d=123	Nys	0.45(0.01)	81.79	88.39(0.00)
	RRLS-Nys	0.54(0.01)	81.82	88.39(0.01)
	SCRF	4.94(0.20)	76.38	77.99(0.09)
	MCM	0.24(0.01)	82.08	86.55(0.02)
Shuttle m=43500 n=14500 d=9	Nys	0.54(0.03)	99.85	99.98(0.00)
	RRLS-Nys	0.89(0.07)	99.85	99.98(0.00)
	SCRF	0.41(0.01)	99.85	99.97(0.00)
	MCM	0.32(0.02)	99.85	99.97(0.00)
Mnist m=60000 n=10000 d=784	Nys	1.20(0.04)	99.31	99.47(0.01)
	RRLS-Nys	2.45(0.06)	99.32	99.47(0.01)
	SCRF	12.79(0.17)	99.31	99.47(0.01)
	MCM	0.46(0.01)	99.39	99.62(0.01)
Vehicle m=78823 n=19705 d=100	Nys	1.32(0.05)	85.37	91.44(0.00)
	RRLS-Nys	1.44(0.03)	85.38	91.45(0.00)
	SCRF	7.70(0.16)	83.92	87.14(0.02)
	MCM	0.56(0.03)	83.92	87.11(0.03)
Skin m=157464 n=87593 d=3	Nys	9.30(0.21)	99.94	99.96(0.00)
	RRLS-Nys	9.20(0.90)	99.94	99.96(0.00)
	SCRF	0.63(0.01)	99.94	99.96(0.00)
	MCM	1.12(0.01)	99.94	1.00(0.00)
Covtype m=456533 n=124479 d=54	Nys	15.96(0.17)	95.14	97.81(0.03)
	RRLS-Nys	13.85(0.58)	95.13	97.81(0.02)
	SCRF	26.80(0.24)	95.17	97.81(0.05)
	MCM	3.36(0.07)	95.15	97.81(0.03)

problem. Then we randomly chose 1000000 points as training samples and the remaining 600000 points as test samples.

In order to analyze the influence of the number of samples on the classification performance of the Nys and RRLS-Nys, we gradually increased the number of sample columns from 100 to 900. Fig. 4 shows the variation of AUC and training time with the number of samples for the MCM, Nys and RRLS-Nys, respectively.

As can be seen from Fig. 4(a), the performance of the Nys and RRLS-Nys improves with the increase of the number of samples. However, the performance of the Nys and RRLS-Nys cannot be comparable to that of MCM until the number of samples is 900. In addition, it can be seen from Fig. 4(b) that the training time of Nys and RRLS-Nys increased significantly with the increase of the sample number, which is much larger than MCM. Based on the above analyses, we conclude that MCM is more suitable for the Checkerboard dataset.

D. Multi-class Classification

In this section, Multi-classification experiments were performed by one-versus-all [40] on the six benchmark multi-classification datasets. In order to compare the performance of the four approximate methods objectively and impartially, we also adopted Macro averaged F1 scores (Macro- F_1) [41] and Matthews correlation coefficient (MCC) [42] as the evaluation criteria. The detailed information of the six benchmark multi-classification datasets are listed in Table VI. And these datasets were downloaded from the LIBSVM [34].

Table VII reports the experimental results for the six benchmark multi-classification datasets.

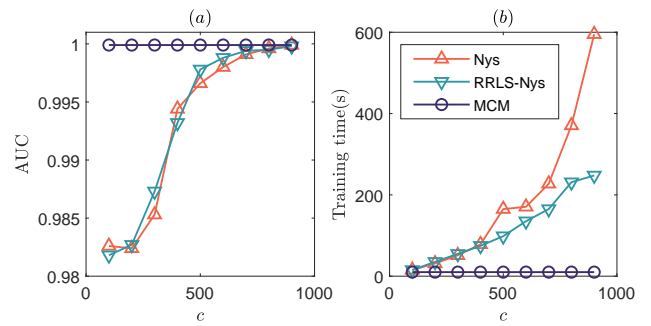


Fig. 4: AUC and training time with different sampling column numbers on the Checkerboard dataset.

TABLE VI: Datasets used in multi-classification experiments.

Data Sets	Classes	Features	Train num.	Test num.
Shuttle	7	9	43500	14500
Sensorless	11	48	46656	11853
Connect-4	3	126	54872	12685
Mnist	10	784	60000	10000
Vehicle	3	100	78823	19705
CovtypeM	7	54	456533	124479

TABLE VII: Comparison of different algorithms on the six benchmark multi-classification datasets. The standard deviations are given in brackets.

Data Sets	Algorithms	Training time(s)	Accuracy (%)	Macro- F_1 (%)	MCC (%)
Shuttle	Nys	5.78(0.10)	99.77	73.81(0.11)	99.35(0.01)
	RRLS-Nys	8.70(0.37)	99.78	74.03(0.50)	99.35(0.01)
	SCRF	3.24(0.05)	99.77	73.76(0.00)	99.35(0.00)
	MCM	2.39(0.06)	99.77	73.76(0.00)	99.35(0.00)
Sensorless	Nys	9.13(0.06)	98.92	98.91(0.01)	98.81(0.11)
	RRLS-Nys	9.81(0.18)	98.91	98.92(0.01)	98.81(0.11)
	SCRF	27.21(0.11)	98.88	98.88(0.01)	98.76(0.01)
	MCM	4.18(0.05)	98.91	98.91(0.01)	98.80(0.01)
Connect-4	Nys	1.53(0.03)	80.94	57.55(0.49)	58.63(0.54)
	RRLS-Nys	2.15(0.05)	80.78	57.45(0.55)	58.50(0.73)
	SCRF	11.97(0.08)	81.37	58.36(0.49)	59.60(0.47)
	MCM	1.33(0.05)	81.71	59.68(0.59)	60.55(0.54)
Mnist	Nys	15.97(0.30)	96.80	96.79(0.00)	96.44(0.00)
	RRLS-Nys	29.24(0.34)	96.80	96.79(0.03)	96.44(0.04)
	SCRF	126.78(0.34)	96.74	96.74(0.01)	96.38(0.02)
	MCM	8.37(0.16)	96.75	96.74(0.00)	96.39(0.00)
Vehicle	Nys	3.08(0.13)	82.77	82.00(0.01)	72.78(0.01)
	RRLS-Nys	3.57(0.27)	82.80	82.02(0.01)	72.82(0.11)
	SCRF	29.32(0.11)	82.77	81.98(0.01)	72.76(0.01)
	MCM	1.77(0.05)	82.76	81.98(0.01)	72.76(0.01)
CovtypeM	Nys	110.75(1.85)	94.08	90.25(0.16)	90.49(0.01)
	RRLS-Nys	92.95(1.85)	94.13	90.27(0.16)	90.56(0.12)
	SCRF	185.39(0.46)	94.03	90.06(0.25)	90.41(0.01)
	MCM	24.21(0.41)	94.09	90.11(0.19)	90.51(0.01)

From Table VII, it can be clearly seen that MCM always has the least time cost, which is consistent with the time complexity. Judging from different evaluation criteria, the classification performance of the four approximate methods is neck and neck. This proves that MCM is more effective to solve the multi-classification problem.

VI. CONCLUSIONS

Kernel Logical Regression (KLR) has a direct probabilistic interpretation and has good performance in many classification problems. However, the time and space complexity is prohibitive for large-scale problems. In this paper, we employ the multilevel circulant matrix (MCM) approximate kernel matrix to save in storage space and accelerate the solution of the KLR. Combined with the characteristics of MCM and our ingenious design, we propose an MCM approximate Newton iterative method. Because MCM's built-in periodicity allows the multidimensional fast Fourier transform (mFFT) to be used in our method, the time complexity and space complexity of each iteration are reduced to $O(n \log n)$ and $O(n)$, respectively. The experimental results show that our method makes KLR scalable for some large-scale binary and multi-classification problems, with less memory consumption, and converges to test accuracy without sacrifice in a shorter time. Therefore, MCM approximate Newton method is a more suitable choice to deal with large-scale classification problems.

REFERENCES

- [1] J. Zhu and T. Hastie, "Kernel logistic regression and the import vector machine," in *Advances in Neural Information Processing Systems*, vol. 14. MIT Press, 2002.
- [2] M. Sugiyama and J. Simm, "A computationally-efficient alternative to kernel logistic regression," in *2010 IEEE International Workshop on Machine Learning for Signal Processing*. IEEE, 2010, pp. 124–129.
- [3] S. S. Keerthi, K. Duan, S. K. Shevade, and A. N. Poo, "A fast dual algorithm for kernel logistic regression," in *ICML*, 2002, pp. 299–306.
- [4] C. Williams and M. Seeger, "Using the Nyström method to speed up kernel machines," in *Advances in Neural Information Processing Systems*, vol. 13. MIT Press, 2001.
- [5] Z. Lei and L. Lan, "Improved subsampled randomized Hadamard transform for linear SVM," in *Proceedings of the AAAI Conference on Artificial Intelligence*, vol. 34, no. 04, 2020, pp. 4519–4526.
- [6] H. Jia, L. Wang, and H. Song, "Large-scale spectral clustering with stochastic Nyström approximation," in *International Conference on Intelligent Information Processing*. Springer, 2020, pp. 26–34.
- [7] Y. Chen and Y. Yang, "Fast statistical leverage score approximation in kernel ridge regression," in *International Conference on Artificial Intelligence and Statistics*. PMLR, 2021, pp. 2935–2943.
- [8] M. Li, W. Bi, J. T. Kwok, and B.-L. Lu, "Large-scale Nyström kernel matrix approximation using randomized SVD," *IEEE Transactions on Neural Networks and Learning Systems*, vol. 26, no. 1, pp. 152–164, 2014.
- [9] D. Calandriello, A. Lazaric, and M. Valko, "Analysis of Nyström method with sequential ridge leverage score sampling," in *Proceedings of the Thirty-Second Conference on Uncertainty in Artificial Intelligence*, 2016, pp. 62–71.
- [10] A. Alaoui and M. W. Mahoney, "Fast randomized kernel ridge regression with statistical guarantees," in *Advances in Neural Information Processing Systems*, vol. 28. Curran Associates, Inc., 2015.
- [11] C. Musco and C. Musco, "Recursive sampling for the Nyström method," in *Advances in Neural Information Processing Systems*, vol. 30. Curran Associates, Inc., 2017.
- [12] S. Kumar, M. Mohri, and A. Talwalkar, "Sampling methods for the Nyström method," *The Journal of Machine Learning Research*, vol. 13, no. 1, pp. 981–1006, 2012.
- [13] A. Gittens and M. W. Mahoney, "Revisiting the Nyström method for improved large-scale machine learning," *The Journal of Machine Learning Research*, vol. 17, no. 1, pp. 3977–4041, 2016.
- [14] A. Rahimi and B. Recht, "Random features for large-scale kernel machines," in *Advances in Neural Information Processing Systems*, vol. 20. Curran Associates, Inc., 2008.
- [15] L. He, N. Ray, Y. Guan, and H. Zhang, "Fast large-scale spectral clustering via explicit feature mapping," *IEEE transactions on cybernetics*, vol. 49, no. 3, pp. 1058–1071, 2019.
- [16] Q. Le, T. Sarlos, and A. Smola, "Fastfood - computing Hilbert space expansions in loglinear time," in *Proceedings of the 30th International Conference on Machine Learning*, ser. Proceedings of Machine Learning Research, vol. 28, no. 3. Atlanta, Georgia, USA: PMLR, 17–19 Jun 2013, pp. 244–252.
- [17] C. Feng, Q. Hu, and S. Liao, "Random feature mapping with signed circulant matrix projection," in *Proceedings of the 24th International Conference on Artificial Intelligence*, 2015, pp. 3490–3496.
- [18] K. Xiong, H. H. C. Iu, and S. Wang, "Kernel correntropy conjugate gradient algorithms based on half-quadratic optimization," *IEEE Transactions on Cybernetics*, pp. 1–14, 2020.
- [19] L. Ding, S. Liao, Y. Liu, L. Liu, F. Zhu, Y. Yao, L. Shao, and X. Gao, "Approximate kernel selection via matrix approximation," *IEEE Transactions on Neural Networks and Learning Systems*, vol. 31, no. 11, pp. 4881–4891, 2020.
- [20] G. Song and Y. Xu, "Approximation of high-dimensional kernel matrices by multilevel circulant matrices," *Journal of Complexity*, vol. 26, no. 4, pp. 375–405, 2010.
- [21] L. Ding and S. Liao, "An approximate approach to automatic kernel selection," *IEEE Transactions on Cybernetics*, vol. 47, no. 3, pp. 554–565, 2017.
- [22] G. Song, "Approximation of kernel matrices in machine learning," Ph.D. dissertation, Department of Mathematics, Syracuse University, Syracuse, NY, USA, 2009.
- [23] L. Ding and S. Liao, "Approximate model selection for large scale LSSVM," in *Asian Conference on Machine Learning*. PMLR, 2011, pp. 165–180.
- [24] R. E. Edwards, H. Zhang, L. E. Parker, and J. R. New, "Approximate l -fold cross-validation with least squares SVM and kernel ridge regression," in *2013 12th International Conference on Machine Learning and Applications*, vol. 1. IEEE, 2013, pp. 58–64.
- [25] L. He and H. Zhang, "Kernel K-means sampling for Nyström approximation," *IEEE Transactions on Image Processing*, vol. 27, no. 5, pp. 2108–2120, 2018.
- [26] R. Yin, Y. Liu, W. Wang, and D. Meng, "Sketch kernel ridge regression using circulant matrix: Algorithm and theory," *IEEE Transactions on Neural Networks and Learning Systems*, vol. 31, no. 9, pp. 3512–3524, 2019.
- [27] J. E. Dennis Jr and R. B. Schnabel, *Numerical Methods for Unconstrained Optimization and Nonlinear Equations*. SIAM, 1996.
- [28] B. Schölkopf, R. Herbrich, and A. J. Smola, "A generalized representer theorem," in *International Conference on Computational Learning Theory*. Springer, 2001, pp. 416–426.
- [29] E. E. Tyrtyshnikov, "A unifying approach to some old and new theorems on distribution and clustering," *Linear Algebra and Its Applications*, vol. 232, pp. 1–43, 1996.
- [30] P. Davis, *Circulant Matrices*. Wiley, 1979.
- [31] S. Boyd, S. P. Boyd, and L. Vandenberghe, *Convex Optimization*. Cambridge university press, 2004.
- [32] M. R. Hestenes and E. Stiefel, "Methods of conjugate gradients for solving linear systems," *Journal of Research of the National Bureau of Standards*, vol. 49, no. 6, 1952.
- [33] G. H. Golub and C. F. Van Loan, *Matrix Computations*. JHU press, 2013.
- [34] C.-J. L. Chih-Chung Chang, "LIBSVM: a library for support vector machines," <https://www.csie.ntu.edu.tw/~cjlin/libSVM/>, 2011.
- [35] D. Dua and C. Graff, "UCI machine learning repository," <http://archive.ics.uci.edu/ml>, 2017.
- [36] T. K. Ho and E. M. Kleinberg, "Building projectable classifiers of arbitrary complexity," in *Proceedings of 13th International Conference on Pattern Recognition*, vol. 2, 1996, pp. 880–885.
- [37] O. Mangasarian and D. R. Musicant, "Lagrangian support vector machines," *The Journal of Machine Learning Research*, vol. 1, pp. 161–177, 2001.
- [38] S. Zhou, "Sparse LSSVM in primal using Cholesky factorization for large-scale problems," *IEEE Transactions on Neural Networks and Learning Systems*, vol. 27, no. 4, p. 783, 2016.
- [39] L. Chen and S. Zhou, "Sparse algorithm for robust LSSVM in primal space," *Neurocomputing*, vol. 275, pp. 2880–2891, 2018.
- [40] V. Vapnik, *The Nature of Statistical Learning Theory*. Springer science & business media, 2013.
- [41] H. Narasimhan, H. Ramaswamy, A. Saha, and S. Agarwal, "Consistent multiclass algorithms for complex performance measures," in *International Conference on Machine Learning*. PMLR, 2015, pp. 2398–2407.
- [42] J. Gorodkin, "Comparing two K-category assignments by a K-category correlation coefficient," *Computational Biology and Chemistry*, vol. 28, no. 5–6, pp. 367–374, 2004.